Original Research Article

The Effect of Metformin on Radiation-Induced Lung Fibrosis in Mice

Dose-Response:
An International Journal
October-December 2024:1–11

DOI: 10.1177/15593258241308051
journals.sagepub.com/home/dos
Sage

Yu-Zhong Chen[1,2,*], Lin Zhao[1,*], Wei Wei[1,*], Jia Gu[1], Zhen-Hua Liu[3], Wen-Yue Shan[1], Jie Dong[1,4], Chao Li[5], Li-Qiang Qin[6], and Jia-Ying Xu[1]

Abstract

Introduction: Radiation-induced lung fibrosis (RILF) is a common complication of thoracic radiotherapy. Metformin has been suggested to have a radioprotective effect. **Objective:** This study explored the radioprotective effects of metformin on RILF and its mechanisms. **Methods:** C57BL/6J mice were randomly divided into control, ionizing radiation (IR), low-dose metformin (L-Met), and high-dose metformin (H-Met) groups. The IR, L-Met, and H-Met groups received 15 Gy chest irradiation. The L-Met and H-Met groups were administrated 100 or 200 mg/kg metformin from 3 days before irradiation and continued for 6 months. The mice were then sacrificed, and samples were collected for further analysis. **Results:** RILF was induced in the irradiated mice. Metformin improved lung pathology, inhibited collagen deposition, and reduced inflammatory factors such as high mobility group box 1 (HMGB1), interleukin-1 beta, interleukin-6, tumor necrosis factor alpha in lung tissue, lavage fluid, and serum. Western blot and quantitative real-time PCR analyses revealed that metformin downregulated HMGB1, toll-like receptor 4 (TLR4), and nuclear factor kappaB (NF-κB) expression. Additionally, metformin reversed the irradiation-induced reduction in the abundance of Lactobacillus and Lachnospiraceae at the genus level. Conclusion: Our findings indicated that metformin ameliorates RILF by downregulating the inflammatory-related HMGB1/TLR4/NF-κB pathway and improving intestinal flora disorder.

Keywords

metformin, radiation, lung fibrosis, inflammatory factors, gut microbiota

Introduction

Lung cancer is the leading cause of cancer-related death worldwide, with an estimated 1.8 million deaths.[1] Thoracic radiotherapy plays a major role in the management of lung cancer, with over 65% of patients receiving this modality at some point during their cancer course.[2] While radiotherapy continues to be a major treatment option, it is associated with

[1] State Key Laboratory of Radiation Medicine and Protection, Collaborative Innovation Center of Radiation Medicine of Jiangsu Higher Education Institutions, School of Radiation Medicine and Protection, Suzhou Medical College of Soochow University, Suzhou, China
[2] Yancheng Municipal Center for Disease Control and Prevention, Yancheng, China
[3] Department of Radiotherapy, The Yancheng Clinical College of Xuzhou Medical University, The First people's Hospital of Yancheng, Yancheng, China
[4] The First Affiliated Hospital of Soochow University, Suzhou, China
[5] Suzhou Kowloon Hospital, Shanghai Jiaotong University School of Medicine, Suzhou, China
[6] Department of Nutrition and Food Hygiene School of Public Health, Suzhou Medical College of Soochow University, Suzhou, China

Received 19 June 2024; accepted 17 November 2024
*Yu-Zhong Chen, Lin Zhao and Wei Wei contributed equally to this work.

Corresponding Author:
Jia-Ying Xu, School of Radiation Medicine and Protection, Suzhou Medical College of Soochow University, 199 Ren'ai Road, Suzhou Industrial Park, Suzhou, 215123, China.
Email: xujiaying@suda.edu.cn

dose-limiting side effects that can severely impact patients' quality of life. Radiation-induced lung fibrosis (RILF) is a common complications of thoracic radiotherapy, with no effective treatment currently available.[2-4] Symptoms of RILF occurs several months after radiotherapy and may persist for up to two years.[3] The main clinical symptoms of RILF include inflammatory infiltration of interstitial fluid, nonproductive cough, progressive dyspnea, and deterioration of pulmonary function, ultimately leading to respiratory failure.[2-5]

High-mobility group box 1 (HMGB1) is an inflammatory factor released passively by necrotic and damaged cells, as well as actively by immune cell activation.[6] It can directly bind to toll-like receptor 4 (TLR4), triggering the release of proinflammatory cytokines.[7] Recent studies have shown that HMGB1 is closely involved in fibrotic disorders, including cystic fibrosis, liver fibrosis, and lung fibrosis, and inhibiting HMGB1 signaling can protect against fibrotic diseases in experimental models.[8] While it have been reported that radiation may induce the release of HMGB1, its specific role in RILF remains unclear.[9]

Gut microbiota dysbiosis not only modulates the function of the gastrointestinal tract but also impacts distal organs, including the lungs. Several studies have found that gut microbiota composition was altered in pulmonary fibrosis associated with systemic sclerosis and silicosis.[10] Although direct evidence linking gut microbiota to the development of RILF is lacking, studies suggest that radiation-induced pneumonia can alter gut bacterial taxonomic proportions, which were reversed by fecal microbiota transplantation.[11] Thus, it is plausible that gut microbiota is involved in RILF characterized by inflammatory infiltration.

Metformin is widely used as the first-line treatment for type 2 diabetes. In addition to its glucose-lowering effects, metformin has other potential health benefits, including anti-inflammatory, anti-oxidant, anti-tumor, immune-regulating, and gut microbiota-regulating properties.[12,13] Previous studies have observed the beneficial effects of metformin on lung fibrosis in murine models established by silica, bleomycin, or radiation.[14-17] However, the exact mechanisms by which metformin benefits RILF are still unclear. Therefore, we investigated the potential radioprotective effects and mechanisms of metformin in RILF, focusing on the HMGB1/TLR4 pathway and gut microbiota regulation.

Materials and Methods

Mouse Grouping and Treatments

A total of 48 six-to-eight-week-old C57BL/6 J mice (20 ± 2 g body weight) were obtained from Shanghai Shrek Company and housed under 12 h/12 h light/dark cycle at a constant temperature of 22 ± 2°C and 60 ± 5% relative humidity. After a one-week of acclimatization period, mice were assigned randomly to the following 4 groups: control group (n = 12), IR group (n = 12), L-Met group (n = 12), and H-Met group (n = 12). Before irradiation, the mice in the L-Met and H-Met groups received daily oral administration of 100 and 200 mg/kg body weight of metformin (TCI Chemical, Shanghai, China), respectively. Metformin were dissolved in the drinking water and dosage used in the study was decided besed on the previous animal studies.[18,19] After 3 days of the administration, the mice in the IR, L-Met, and H-Met groups were anesthetized using chloral hydrate (0.06 mL/10 g), and the whole chest (the rest of the body parts were adequately shielded) was exposed to a single dose of 15 Gy in the supine position using a medical linear accelerator with 6 MeV at a dose rate of 300 cGy/min. The source skin distance was 100 cm, and the irradiation field was 2 cm × 40 cm. The mice in the control group exposed to sham radiation. After irradiation, the mice in the L-Met and H-Met groups were gavaged metformin solution 5 days a week for 6 months. The mice in the control and IR groups were orally administered saline. The mice were monitored daily for any sign of mortality (if any) and weekly for body weight (BW) throughout the experimental period. The care and use of laboratory animals followed to the guidelines for Animal Experiments of Soochow University and adhered to the recommendations of International Council for Laboratory Animal Science.

Sample Collection

The experiment was ended after 6 months of radiation exposure. After an overnight fasting, the mice were anesthetized and peripheral blood was obtained from the orbital sinus to obtain serum. Then, a tracheotomy was performed. The trachea was inserted and lavaged twice with 1 mL of sterile saline. The recovered fluids were filtered through a single layer of gauze to remove the mucus, and bronchoalveolar lavage fluid (BALF) was collected.[20] The serum and BALF were frozen at −80°C for later use. Lung tissues were removed and lung wet weight (LWW) was recorded.[21] The right lung was frozen immediately at −80°C, and the left parts were fixed in 10% neutral buffered formalin. The intestinal contents were collected for the detection of gut microbiota.

Determination of Inflammatory Cytokines of Lung Tissue, BALF, and Serum

The frozen lung tissue samples were homogenized for 10 min and centrifuged for 10 min at 3000 r/min at 4°C to get the supernatants. The levels of inflammatory cytokines HMGB1, interleukin-1 beta (IL-1β), interleukin-6 (IL-6), and tumor necrosis factor alpha (TNF-α) in the supernatants of lung tissue, BALF, and serum were quantified using enzyme-linked immunosorbent assay (ELISA) according to the kit instructions (ColorfulGene, Wuhan, China).

Histopathological Examination of Lung

Formalin-fixed lung was embedded in paraffin and cut into 5 μm slices. After deparaffinized, sections were assessed by

routine hematoxylin-eosin (HE) staining. The pathological score was performed using a semiquantitative scoring system under a Leica DMi8 light microscope (Leica, Weztlar, Germany).[22] Masson staining was performed on the deparaffinized sections using Masson dye solution, and the degree of fibrosis was evaluated according to Ashcroft fibrosis score.[23]

Immunohistochemistry Assay of Lung

Deparaffinized lung tissue sections were rehydrated through a graded series of ethanol and treated with 3% H_2O_2 to quench endogenous peroxidase activity. They were incubated overnight at 4°C with rabbit polyclonal antibody against Collagen-I (1:1000; Proteintech, IL, USA), Samd2 (1:500; Servicebio, Wuhan, China), and TGF-β1 (1:200; Proteintech, IL, USA), and then with goat anti-rabbit secondary antibody (1:50; Beyotime Institute of Biotechnology, Haimen, China). Diaminobenzidine was used as the chromogen to observe immunohistochemical positive cells in randomly selected 5 fields of view. The images are quantitatively calculated with Image Pro Plus image analysis software.

Quantitative Real-Time Polymerase Chain Reaction (qPCR) Analysis in Lung Tissues

According to the manufacturer's protocol, RNA was extracted from the homogenized left lung tissue using the TRIzol reagent (Tiangen Biotech, Beijing, China). The quantification and qualitative ratiometric analysis of RNA were performed using a Nanodrop 2000 (Thermo Fisher Scientific, MA, USA). For each sample, 1 μg of total RNA was reverse-transcribed with a High-Capacity cDNA Reverse Transcription kit (Thermo Fisher Scientific, MA, USA). The qPCR primers were designed using primer BLAST, and the sequences are shown in Table 1. The target genes were identified using a ChamQ™ Universal SYBR green PCR master mix (Vazyme Biotech, Nanjing, China) on a QuantStudio™ 6 Flex system (Thermo Fisher Scientific, MA, USA). The levels of mRNA were normalized to GAPDH transcripts using the $2^{-\Delta\Delta Ct}$ method.

Western Blot Analysis in Lung Tissues

Frozen lung tissues were homogenized in ice-cold lysis buffer. The supernatants were collected after centrifugation. Protein concentration was measured according to the bicinchoninic acid protein assay kit (Beyotime Institute of Biotechnology, Haimen, China). After denaturation, an equal amount of protein (50 μg) was separated by 10% SDS-PAGE and transferred to a PVDF membrane. The membranes were blocked with 5% skim milk in Tris-buffered saline Tween-20 solution for 1 h and then were incubated overnight with appropriate primary antibodies at 4°C. The antibodies included HMGB1 (1:1000), TLR4 (1:1000), NF-κB (1:2000), myeloid differential protein-88 (MyD88, 1:1000), inhibitor of kappa B kinase β (IKKβ, 1:1000), and IL-1β (1:1000). The first 3 antibodies were obtained from Proteintech (IL, USA) and the last 3 from Cell Signaling Technology (MA, USA). After being washed 3 times in phosphate buffered saline with Tween-20 and incubated with appropriate secondary antibodies. Membranes were developed by chemiluminescence using Superstar ECL Western Blotting Substrate reagents (Beyotime Institute of Biotechnology, Haimen, China). The band intensities were quantified using Image J software (https://imagej.net/).

Table 1. Primers Used in This Study.

Target	Primer Sequence (5′ to 3′)
TLR4 F	GTTGCAGAAAATGCCAGGATG
TLR4 R	CAGGGATTCAAGCTTCCTGGT
NF-κB F	ACGACATTGAGGTTCGGTTC
NF-κB R	ATCTTGTGATAGGGCGGTGT
HMGB1 F	CAGCCATTGCAGTACATTGAGC
HMGB1 R	TCTCCTTTGCCCATGTTTAGTTG
IL-6 F	TAGTCCTTCCTACCCCAATTTCC
IL-6 R	TTGGTCCTTAGCCACTCCTTC
TNF-α F	CCTGTAGCCCACGTCGTAG
TNF-α R	GGGAGTAGACAAGGTACAACCC
IL-1β F	GCAACTGTTCCTGAACTCAACT
IL-1β R	ATCTTTTGGGGTCCGTCAACT
GAPDH F	TGGATTTGGACGCATTGGTC
GAPDH R	TTTGCACTGGTACGTGTTGAT

Bacterial Diversity Analysis

Gut microbiota was analyzed using 16S rRNA gene sequencing in an Illumina NovaSeq platform (Lc-Bio Technologies, Hangzhou, China).

Statistical Analysis

All data are expressed as the mean ± standard deviation (SD). Differences among the groups were tested by one-way analysis of variance (ANOVA) followed by the LSD post hoc test. Statistical analysis was performed with IBM SPSS Statistics for Windows, version 24 (IBM Corp., Armonk, NY, USA). The differences were considered statistically significant when $P < 0.05$.

Results

Effects of Metformin on Body and Lung Weights

No mortality was observed during the experiment. After radiation, mice appeared listless and transient reduction in food intake and body weight, which gradually recovered within

3 days. No significant differences in body weights were observed among the groups. After 3 months, the mice in the IR group appeared to have albinism of hair and hair loss, which were not such obvious in both metformin treatment groups (Figure 1A and B). LWW/BW reflects the severity of lung vascular permeability and lung edema. Compared with the control group, LWW/BW was significantly increased in the IR group and was reduced in the metformin treatment groups (Figure 1C and D).

Metformin Protected Mice from Radiation-Induced Lung Fibrosis

HE staining observed normal structure of lung tissue in the control group. While the IR group exhibited significant pathological changes including thickened alveolar walls and fused fibrous tissues in the alveolar space. Pulmonary interstitial was broadened with visible muscle fibroblast hyperplasia. Bronchi and blood vessels were surrounded by fibrous tissues and infiltrated with inflammatory cells. These changes were improved in both metformin treatment groups, which were further supported by the pathological scores of lung tissue (Figure 2A). Compared with the control group, Masson staining showed that collagen deposition, an important indicator of lung fibrosis, was more pronounced in the IR group. In contrast, collagen deposition was ameliorated in metformin treatment groups. Quantitatively, the fibrosis scores were significantly lower in the L-Met (4.20 ± 0.84) and H-Met (3.00 ± 1.00) groups than in the IR group (6.40 ± 1.14), and further significantly decreased in the H-Met group compared with the L-Met group (Figure 2B).

Immunohistochemical staining identified strong positive cells of collagen-I, Samd2, and TGF-β1 in the IR group, whereas relatively fewer positive cells were observed in the metformin treatment groups. Semiquantitative analysis showed that Samd2 positive cells in the L-Met group and positive cells of all 3 markers in the H-Met group were significantly decreased compared with the IR group. Additionally, Samd2 and TGF-β1 positive cells were significantly lower in the H-Met group than in the L-Met group (Figure 3A-C). Similar results were observed in the Western blot analyses. The protein expression of all 3 markers was upregulated in the IR group compared with the control group. The protein expressions of Samd2 (in the L-Met group) and all 3 markers (in the H-Met group) were significantly downregulated compared with the IR group (Figure 3D).

Metformin Suppressed Radiation-Induced Inflammation Response

In lung tissues, the levels of inflammatory factors (HMGB1, IL-1β, IL-6, and TNF-α) were significantly increased by irradiation. Compared with the IR group, TNF-α levels in the L-Met group and HMGB1, IL-1β, and TNF-α levels in the H-Met group were significantly decreased. Furthermore, HMGB1 levels were significantly lower in the H-Met group than in the L-Met group (Figure 4A). In BALF, irradiation significantly increased HMGB1 and IL-6 levels. Compared with the IR group, TNF-α levels in the L-Met group and HMGB1 and IL-6 levels in the H-MET group were significantly decreased (Figure 4B). In serum, the levels of all inflammatory factors were increased by irradiation. Compared with the IR group, HMGB1 levels in the L-Met group and HMGB1, IL-6, and TNF-α levels in the H-Met group were significantly decreased (Figure 3C).

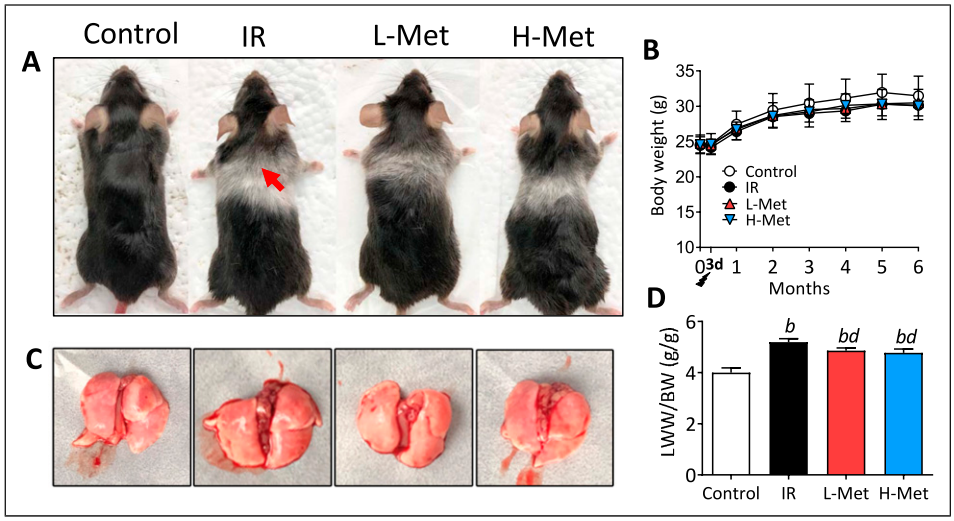

Figure 1. Metformin effects on body and lung weights. (A) Mice appearance and chest albinism, red arrow: white fur; (B) The curve of body weight during the experiments; (C) The anatomy of lung tissue; (D) The lung wet weight to body weight ratio (LWW/BW) among the groups. The results are presented as mean ± SD. $^{b}P < 0.01$ vs Control group, $^{d}P < 0.01$ vs IR group.

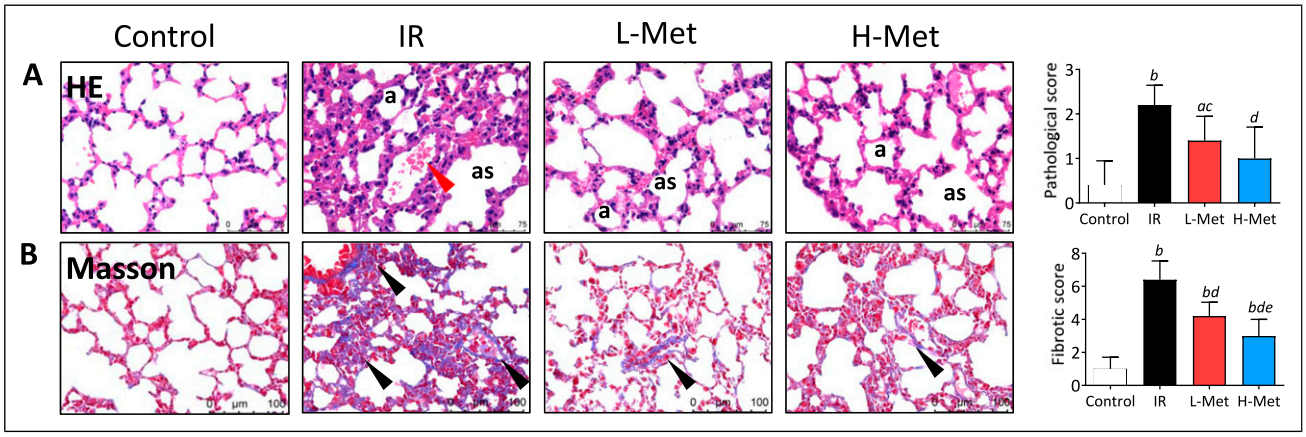

Figure 2. Metformin improved radiation-induced pathological changes in the lungs. (A) Representative images of hematoxylin-eosin staining and the comparison of pathological scores, a: alveolus, as: alveolar septa, red arrow: alveolar hemorrhage; (B) Representative images of Masson's Trichrome staining and the comparison of fibrotic scores, black arrow: thickening of alveolar septa. The results are presented as mean ± SD. $^{a}P < 0.05$ vs Control group, $^{b}P < 0.01$ vs Control group, $^{c}P < 0.05$ vs IR group, $^{d}P < 0.01$ vs IR group, $^{e}P < 0.05$ vs L-Met group.

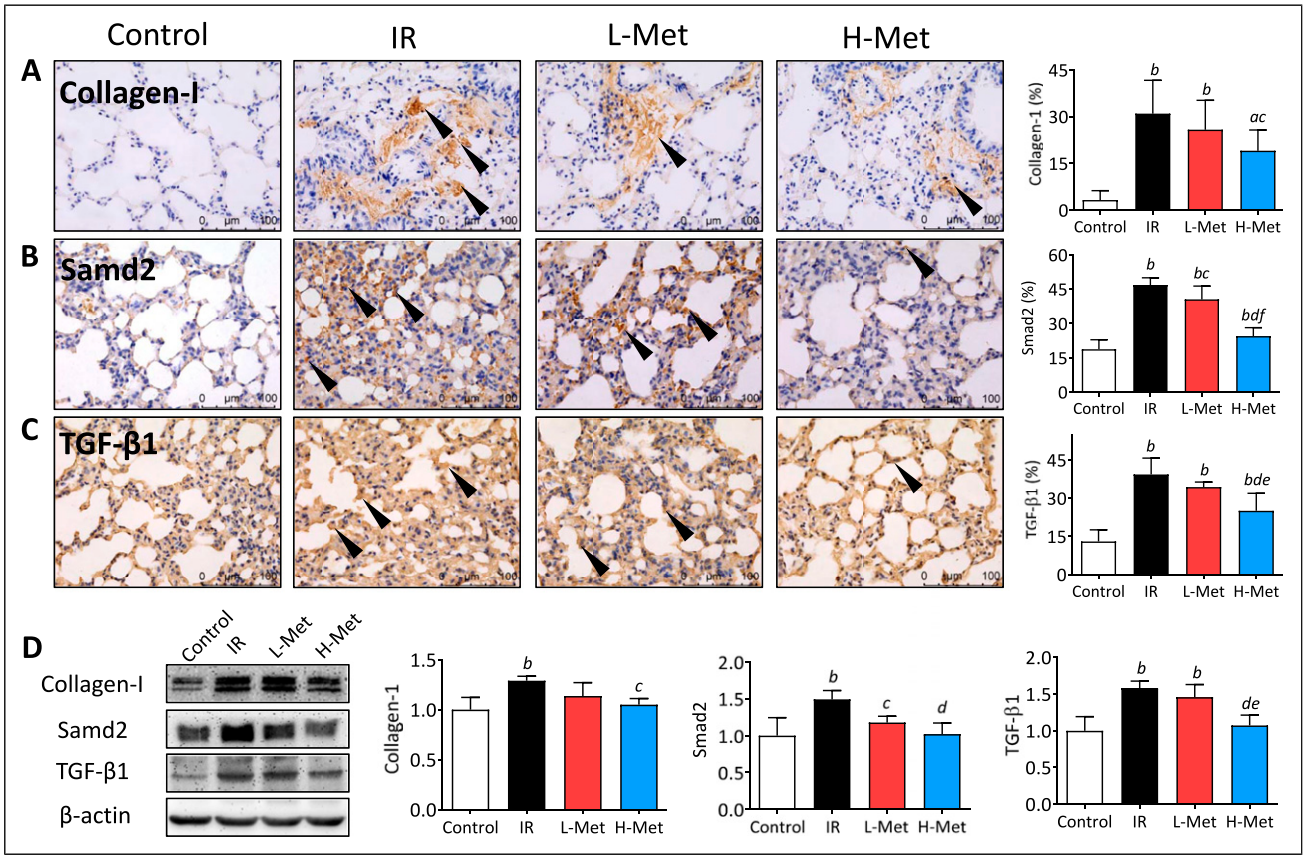

Figure 3. Metformin mitigated radiation-induced lung fibrosis. (A)-(C) Representative images (40×) of immunohistochemical staining of Collagen-I, Samd2, and TGF-β1 and the percentages of their positive cells, black arrow: Collagen-I, Samd2, and TGF-β1 posotive cells. (D) Representative images of western blot of Collagen-I, Samd2, and TGF-β1 and their quantified calculation of protein expression. The results are presented as mean ± SD. $^{a}P < 0.05$ vs Control group, $^{b}P < 0.01$ vs Control group, $^{c}P < 0.05$ vs IR group, $^{d}P < 0.01$ vs IR group, $^{e}P < 0.05$ vs L-Met group, $^{f}P < 0.01$ vs L-Met group.

Metformin Reduced Inflammation Response via HMGB1/TLR4/NF-κB Pathway

The protein expression levels of HMGB1, TLR4, IKKβ, NF-κB, MyD88, and IL-1β were significantly upregulated by irradiation. Compared with the IR group, the protein expression levels were significantly downregulated in the metformin treatment groups (Figure 5A). Similarly, the mRNA expression levels of HMGB1, TLR4, and NF-κB were significantly upregulated by irradiation. Compared with the IR group, the mRNA expression levels of HMGB1 and NF-κB were significantly downregulated in the metformin treatment groups (Figure 5B).

Metformin Improved Intestinal Bacterial Flora Structures

The observed species and Chao1 index were used to estimate the operational taxonomic unit (OUT) numbers, and the Shannon index was used to evaluate the microbial diversity. No significant differences were observed among the four groups (Figure 6A-C). Principal coordinate analysis (PCA) showed that intestinal bacterial flora structures were substantially changed after irradiation (Figure 6D). Unweighted Principal component analysis (PCoA) analysis indicated that intestinal bacterial flora structures in the metformin treatment groups were close to the control group (Figure 6E). At the genus level, IR significantly reduced the relative abundance of Lactobacillus and Lachnospiraceae- NK4A136 group bacteria. Compared with the IR group, Lactobacillus was significantly increased in the H-Met group, and Lachnospirace was significantly increased in both metformin treatment groups. Lactobacillus was further significantly increased in the H-Met group compared with the L-Met group (Figure 6F–I).

Discussion

RILF is a chronic, progressive lung disease with limited treatment options that severely affect patients' quality of life.[3] Lung fibrosis is characterized by fibroblast proliferation and the abnormal accumulation of fibrillar collagens promoted by TGF-β1 activation. After binding to the TGF-β receptor, TGF-β1 phosphorylates Smad proteins, promoting collagen synthesis and inducing myofibroblast formation.[24,25] We monitered that the production of collagen-I, Samd2, and TGF-β1 in RILF was significantly inhibited by metformin. Wang et al. observed that metformin treatment for 12 weeks significantly decreased collagen-1a, TGF-β, and p-Smad2 expression in

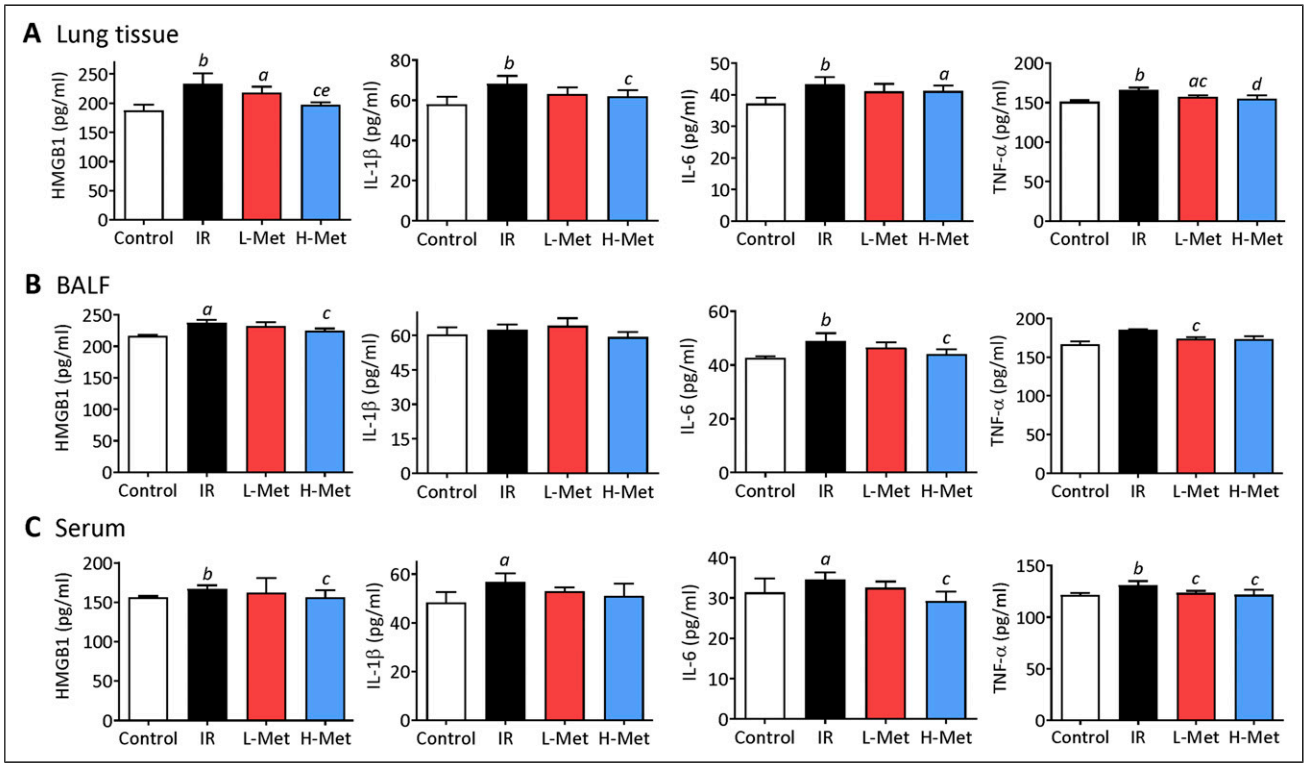

Figure 4. Metformin suppressed radiation-induced inflammation response in lung tissue, bronchoalveolar lavage fluid (BALF) , and serum. (A) The production of cytokines high-mobility group box 1 (HMGB1), interleukin-1 beta (IL-β1), interleukin-6 (IL-6), and tumor necrosis factor alpha (TNF-α) in the lung tissue. (B) Cytokines levels in bronchoalveolar lavage fluid (BALF). (C) Cytokines levels in serum. The results are presented as mean ± SD. $^{a}P < 0.05$ vs Control group, $^{b}P < 0.01$ vs Control group, $^{c}P < 0.05$ vs IR group, $^{d}P < 0.01$ vs IR group, $^{e}P < 0.05$ vs L-Met group.

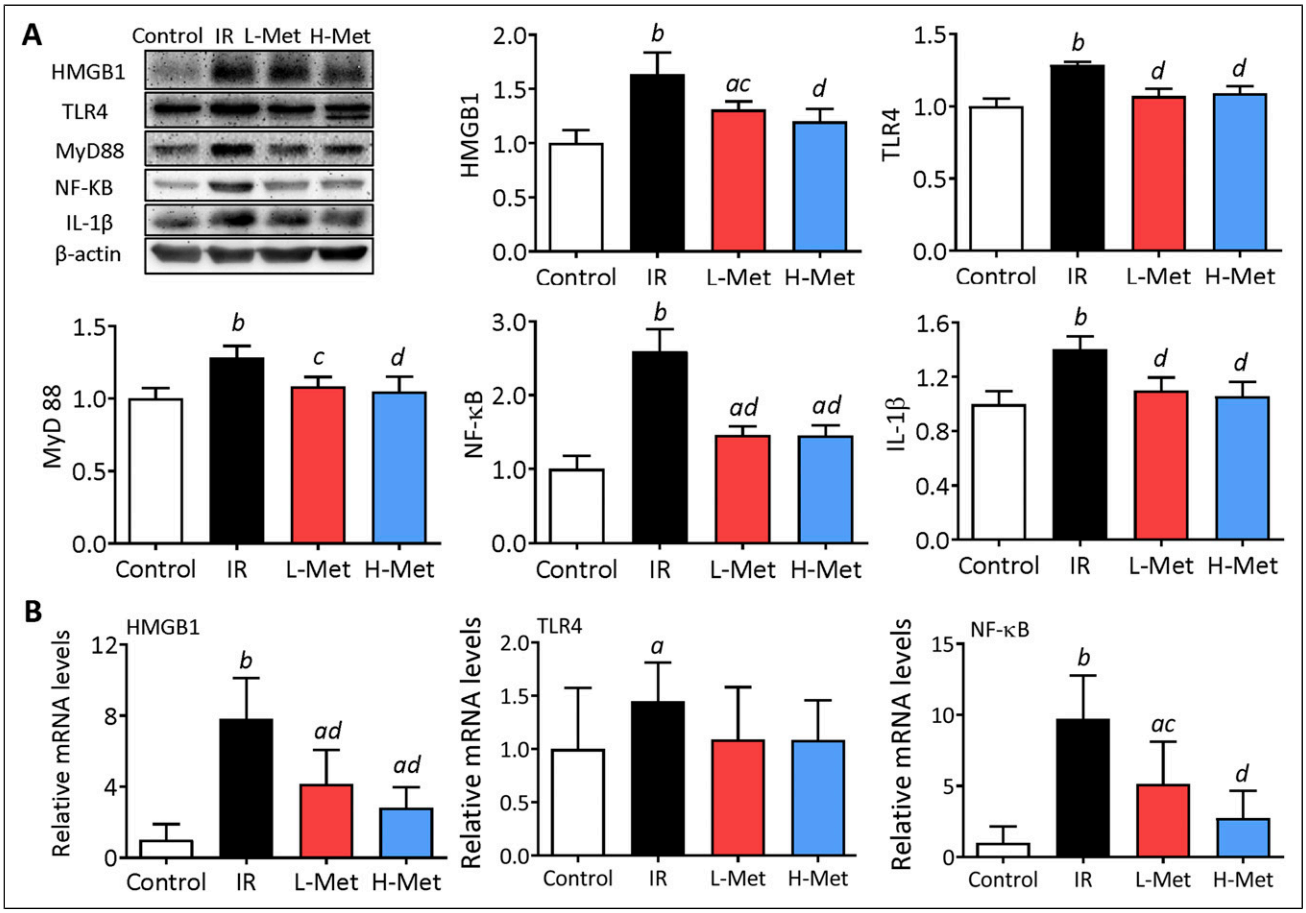

Figure 5. Metformin reduced inflammation response via high-mobility group box 1(HMGB1)/toll-like receptor 4 (TLR4)/nuclear factor kappa B (NF-κB) pathway in the lung tissue. (A) Representative images of western blot of HMGB1, TLR4, myeloid differentiation primary response protein 88 (MyD88), NF-κB, and interleukin-1 beta in the lung tissues and their quantified calculation of protein expression. (B) mRNA expression levels of HMGB1, TLR4, and NF-κB in lung tissues. The results are presented as mean ± SD. $^{a}P < 0.05$ vs Control group, $^{b}P < 0.01$ vs Control group, $^{c}P < 0.05$ vs IR group, $^{d}P < 0.01$ vs IR group.

rats received whole lung 20 Gy irradiation.[17] Thus, metformin can alleviate radiation-induced lung fibrosis by inhibiting collagen deposition and ameliorating pathological changes.

Radiation-induced lung injury involves several mechanisms, with the primary one being an increased inflammatory response. Proinflammatory cytokine HMGB1 significantly enhances collagen deposition, stimulates fibroblast proliferation, and participates in fibrogenesis.[26] Hamada et al. found that HMGB1 levels in BALF and lung tissues were significantly higher in pulmonary fibrosis patients than in normal ones.[20] We found that irradiation increased HMGB1 levels in lung tissue, BALF, and serum, indicating its involvement in the early inflammatory process of RILF. However, metformin treatment, especially at high doses, inhibited the production of HMGB1. Cytokines play multiple roles in the process of RILF.[27] Anti-HMGB1 antibody treatment significantly decreased the expression levels of TNF-α, IL-6, and IL-17 in BALF of irradiated mice.[28] Additionally, we found that metformin reduced the release of inflammatory factors IL-1β, IL-6, and TNF-α in irradiated mice. Gamad et al also found that metformin treatment inhibited inflammatory cells and inflammatory mediators (TNF-α and IL-6) in BALF and improved bleomycin-induced pulmonary fibrosis in rats.[16]

Several studies have shown that HMGB1 can bind to TLR4 receptors and activate NF-κB nuclear translocation to induce lung fibrosis.[29-31] Wang et al found that HMGB1 activated NF-κB and released TGF-β1, α-SMA, and collagen-I in human lung fibroblasts in vitro. These HMGB1-induced expressions of TGF-β1, α-SMA, and collagen-I in lung fibroblasts were blocked by inhibiting NF-κB activation.[31] Furthermore, radiation-exposed macrophages have been shown to secrete HMGB1 to activate NF-κB through binding to TLR4, leading to an inflammatory response.[32] These studies suggested that HMGB1 plays a crucial role in mediating RILF and HMGB1/TLR4/NF-κB pathway is a key signaling pathway to mediate RILF.[33] As expected, radiation exposure significantly upregulated the expression of HMGB1, TLR4, and NF-κB at both protein and gene levels. Metformin significantly inhibited the HMGB1/TLR4/NF-κB

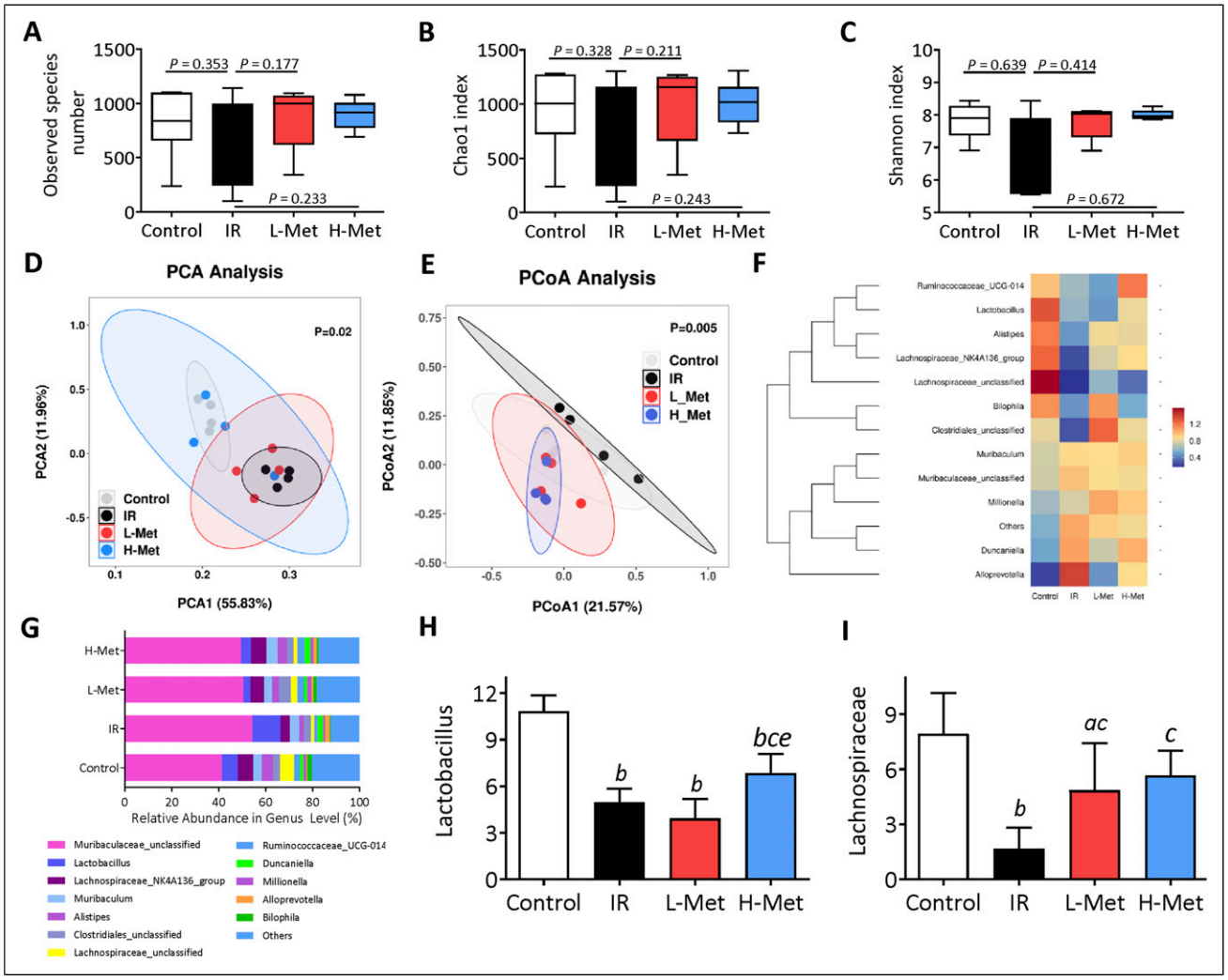

Figure 6. The effects of metformin on intestinal gut microbiota. (A)-(C) The indexes of the abundance and diversity of intestinal gut microbiota bacterial, including the observed species number, Chao1 index, and Shannon index. (D) Principal coordinate analysis (PCA) of gut microbiomes. (E) Principal component analysis (PCoA) of gut microbiomes. (F) The differences in intestinal bacterial structure at the genus level among the groups (G) The relative abundance of bacterial flora at the genus level. (H) The relative abundance of lactobacillus. (I) The relative abundance of Lachnospiraceae-NK4A136. The results are presented as mean ± SD. $^{a}P < 0.05$ vs Control group, $^{b}P < 0.01$ vs Control group, $^{c}P < 0.05$ vs IR group, $^{e}P < 0.05$ vs L-Met group.

pathway and TLR4 downstream of MyD88 expression and subsequently proinflammatory cytokine IL-1β. These findings were also supported by changes in inflammatory factors detected in the lung tissue, BALF, and serum. Collectively, these results suggest that metformin may inhibit inflammation to alleviate RILF via the HMGB1/TLR4/NF-κB pathway in irradiated mice.

Clinical trials and animal experiments have shown a complex response in radiation-induced RILF.[2,4,34] Intestinal microbial disturbance can also affect the efficacy of radiotherapy.[35] Preclinical studies has indicated that metformin play an important role in gut microbiome modulation, including increasing the proportion of parts of the microbiome.[36] We found that intestinal flora community structures by metformin treatment was close to the control group. Furthermore, metformin reversed the reduction in the abundance of Lactobacillus and Lachnospiraceae. Chioma et al. found that Lactobacilli supernatant reduced collagen-1 production in IL-17A-and TGFβ1-stimulated human lung fibroblasts.[37] In CCl_4-treated mice, metformin treatment increased Lactobacillus sp. MF-1 in the feces, while daily gavage of Lactobacillus maintained gut integrity and reduced liver fibrosis.[38] Lachnospiraceae are obligate anaerobes abundant in the human intestine, which affect host health by producing short-chain fatty acids and promoting colonization resistance to intestinal pathogens.[39] Lachnospiraceae is associated with the recovery of hematopoietic function and gastrointestinal repair and can protect against radiation-induced damage in mice.[40] Thus, metformin may exert radioprotective effects via gut

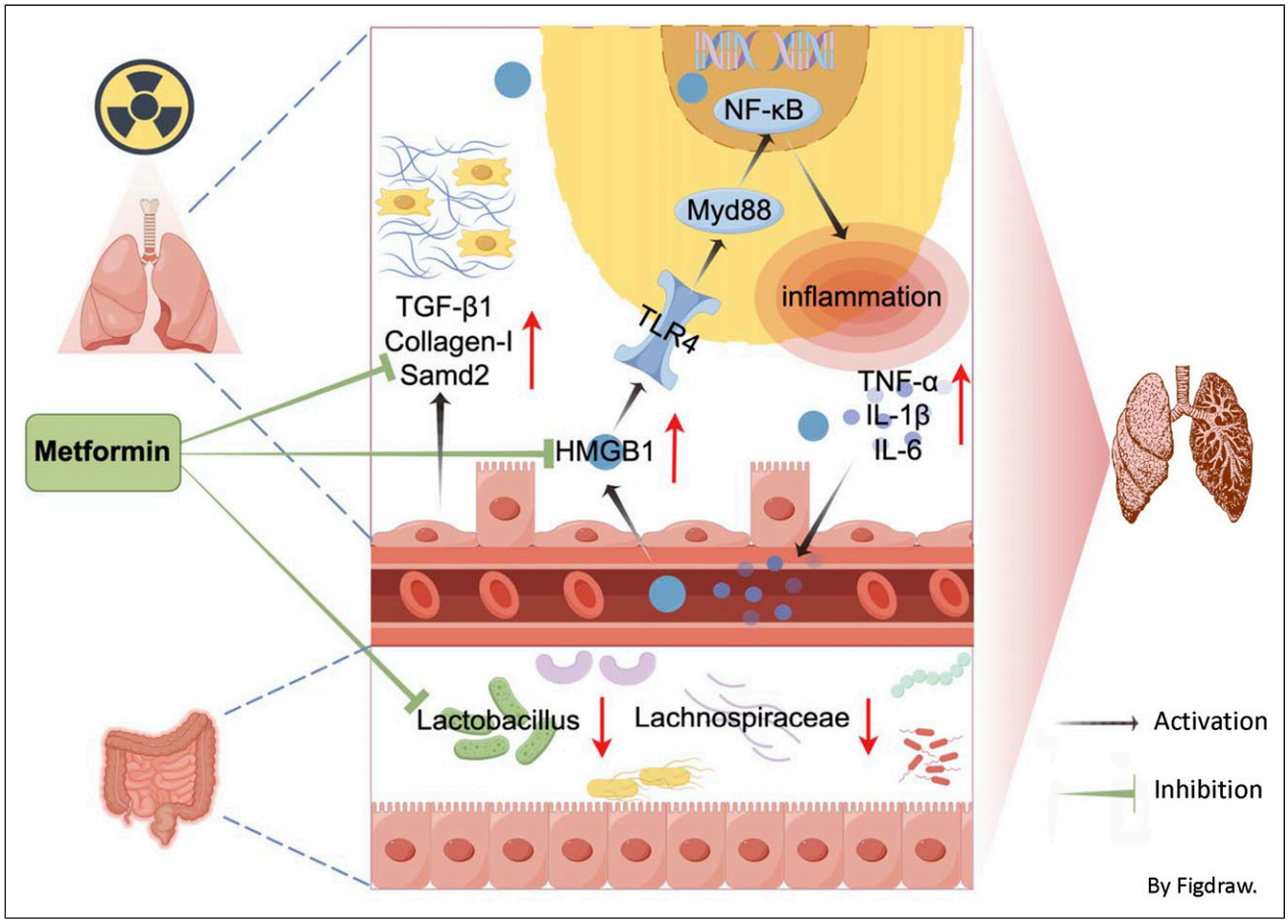

Figure 7. Potential mechanisms of radiation-induced lung fibrosis mitigation by metformin. Draw by Figdraw.

microbiome modulation, particularly by regulating the relative abundance of Lactobacillus and Lachnospiraceae in the intestinal tract.

There are some limitations in this animal study. Fisrt, the metformin dose we used was based on the other animal studies. It exceed clinically relevant levels, which may cast doubt on the actual effects of metformin on RILF in clinical practice.[41,42] Second, the sample size was not calculated and justiciaed before the experiment. Third, the favorable effects of metformin were somewhat stronger in the H-Met group than in the L-Met group. However, further robust evidence is needed to determine whether metformin may affect RILF in a dose-dependent manner.

Conclusion

Metformin treatment improves RILF in mice, potentially through the inhibition of fibrosis factor activity, down-regulation of inflammatory-related HMGB1/TLR4/NF-κB pathway, and modulation of gut microbiota (Figure 7). This suggests metformin may offer a novel strategy fore-nhancinging therapeutic effects in RILF.

Appendix

Abbreviations

RILF	Radiation-induced lung fibrosis
IR	Ionizing radiation
L-Met	Low dose metformin
H-Met	High dose metformin
HMGB1	High-mobility group box 1
TLR4	Toll-like receptor 4
BALF	Bronchoalveolar lavage fluid
LWW	Lung wet weight

Author contributions

Yu-zhong Chen: Investigation (equal); methodology (equal); formal analysis (equal); data curation (equal); validation (equal); visualization (equal); writing – original draft (equal). Lin Zhao: Investigation (equal); methodology (equal); validation (equal); writing-original draft (equal). Wei Wei: Investigation (equal); methodology (equal); validation (equal); writing – original draft (equal). Jia Gu: Investigation (equal); methodology (equal). Zhen-Hua Liu: Methodology (equal). Wen-Yue Shan: Investigation (equal). Jie Dong: Investigation (equal). Chao Li: Methodology (equal). Li-Qiang Qin:

Methodology (equal); writing – review and editing (equal). Jia-Ying Xu: Conceptualization (lead); methodology (equal); formal analysis (equal); data curation (equal); supervision (lead); writing – review and editing (equal); validation (lead)

Declaration of conflicting interests

The author(s) declared no potential conflicts of interest with respect to the research, authorship, and/or publication of this article.

Funding

The author(s) disclosed receipt of the following financial support for the research, authorship, and/or publication of this article: This work was financially supported by the National Natural Science Foundation of China (No. 82073482, 81673101, 81703159), Interdisciplinary Basic Frontier Innovation Program of Suzhou Medical College of Soochow University (No. YXY2304035), the Project of State Key Laboratory of Radiation Medicine and Protection, Soochow University (No. GZK12024043).

Ethical Statement

Ethical Approval

All the experimental protocol in this study was approved by the Soochow University Animal Welfare Committee (No. 201903A035) dated March 8, 2019.

ORCID iD

Wei Wei https://orcid.org/0009-0007-6776-4178

References

1. Bray F, Laversanne M, Sung H, et al. Global cancer statistics 2022: GLOBOCAN estimates of incidence and mortality worldwide for 36 cancers in 185 countries. *CA A Cancer J Clin*. 2024;74(3):229-263. doi:10.3322/caac.21834
2. Chen Z, Wu Z, Ning W. Advances in molecular mechanisms and treatment of radiation-induced pulmonary fibrosis. *Transl Oncol*. 2019;12(1):162-169. doi:10.1016/j.tranon.2018.09.009
3. Jin H, Yoo Y, Kim Y, Kim Y, Cho J, Lee YS. Radiation-induced lung fibrosis: PreclinicalAnimal models and therapeutic strategies. *Cancers*. 2020;12(6):1561. doi:10.3390/cancers12061561
4. Hanania AN, Mainwaring W, Ghebre YT, Hanania NA, Ludwig M. Radiation-induced lung injury: assessment and management. *Chest*. 2019;156(1):150-162. doi:10.1016/j.chest.2019.03.033
5. Zanoni M, Cortesi M, Zamagni A, Tesei A. The role of mesenchymal stem cells in radiation-induced lung fibrosis. *Int J Mol Sci*. 2019;20(16):3876. doi:10.3390/ijms20163876
6. Stros M. HMGB proteins: interactions with DNA and chromatin. *Biochim Biophys Acta*. 2010;1799(1-2):101-113. doi:10.1016/j.bbagrm.2009.09.008
7. Yang H, Wang H, Ju Z, et al. MD-2 is required for disulfide HMGB1-dependent TLR4 signaling. *J Exp Med*. 2015;212(1):5-14. doi:10.1084/jem.20141318
8. Li LC, Gao J, Li J. Emerging role of HMGB1 in fibrotic diseases. *J Cell Mol Med*. 2014;18(12):2331-2339. doi:10.1111/jcmm.12419
9. Zheng L, Zhu Q, Xu C, et al. Glycyrrhizin mitigates radiation-induced acute lung injury by inhibiting the HMGB1/TLR4 signalling pathway. *J Cell Mol Med*. 2020;24(1):214-226. doi:10.1111/jcmm.14703
10. Wu Y, Li Y, Luo Y, et al. Gut microbiome and metabolites: the potential key roles in pulmonary fibrosis. *Front Microbiol*. 2022;13:943791. doi:10.3389/fmicb.2022.943791
11. Chen ZY, Xiao HW, Dong JL, et al. Gut microbiota-derived PGF2α fights against radiation-induced lung toxicity through the MAPK/NF-κB pathway. *Antioxidants*. 2021;11(1):65. doi:10.3390/antiox11010065
12. Dutta S, Shah RB, Singhal S, et al. Metformin: a review of potential mechanism and therapeutic utility beyond diabetes. *Drug Des Dev Ther*. 2023;17:1907-1932. doi:10.2147/DDDT.S409373
13. Pavlo P, Kamyshna I, Kamyshnyi A. Effects of metformin on the gut microbiota: a systematic review. *Mol Metabol*. 2023;77:101805. doi:10.1016/j.molmet.2023.101805
14. Cheng D, Xu Q, Wang Y, et al. Metformin attenuates silica-induced pulmonary fibrosis via AMPK signaling. *J Transl Med*. 2021;19(1):349. doi:10.1186/s12967-021-03036-5
15. Rangarajan S, Bone NB, Zmijewska AA, et al. Metformin reverses established lung fibrosis in a bleomycin model. *Nat Med*. 2018;24(8):1121-1127. doi:10.1038/s41591-018-0087-6
16. Gamad N, Malik S, Suchal K, et al. Metformin alleviates bleomycin-induced pulmonary fibrosis in rats: pharmacological effects and molecular mechanisms. *Biomed Pharmacother*. 2018;97:1544-1553. doi:10.1016/j.biopha.2017.11.101
17. Wang J, Wang Y, Han J, et al. Metformin attenuates radiation-induced pulmonary fibrosis in a murine model. *Radiat Res*. 2017;188(1):105-113. doi:10.1667/RR14708.1
18. Haleh V, Rameshrad M, Najafi M, et al. Cardioprotective effect of metformin in lipopolysaccharide-induced sepsis via suppression of toll-like receptor 4 (TLR4) in heart. *Eur J Pharmacol*. 2016;772:115-123. doi:10.1016/j.ejphar.2015.12.030
19. Adedeji HA, Ishola IO, Adeyemi OO. Novel action of metformin in the prevention of haloperidol-induced catalepsy in mice: potential in the treatment of Parkinson's disease? *Prog Neuro-Psychopharmacol Biol Psychiatry*. 2014;48:245-251. doi:10.1016/j.pnpbp.2013.10.014
20. Hamada N, Maeyama T, Kawaguchi T, et al. The role of high mobility group box1 in pulmonary fibrosis. *Am J Respir Cell Mol Biol*. 2008;39(4):440-447. doi:10.1165/rcmb.2007-0330OC
21. Hu S, Li J, Xu X, et al. The hepatocyte growth factor-expressing character is required for mesenchymal stem cells to protect the lung injured by lipopolysaccharide *in vivo*. *Stem Cell Res Ther*. 2016;7(1):66. doi:10.1186/s13287-016-0320-5
22. Zhang J, Cui R, Feng Y, et al. Serotonin exhibits accelerated bleomycin-induced pulmonary fibrosis through TPH1 knockout mouse experiments. *Mediat Inflamm*. 2018;2018:7967868. doi:10.1155/2018/7967868

23. Ashcroft T, Simpson JM, Timbrell V. Simple method of estimating severity of pulmonary fibrosis on a numerical scale. *J Clin Pathol*. 1988;41(4):467-470. doi:10.1136/jcp.41.4.467
24. Evans RA, Tian YC, Steadman R, Phillips AO. TGF-beta1-mediated fibroblast-myofibroblastterminal differentiation-the role of Smad proteins. *Exp Cell Res*. 2003;282(2):90-100. doi:10.1016/s0014-4827(02)00015-0
25. Hu HH, Chen DQ, Wang YN, et al. New insights into TGF-β/Smad signaling in tissue fibrosis. *Chem Biol Interact*. 2018;292:76-83. doi:10.1016/j.cbi.2018.07.008
26. Lee WJ, Song SY, Roh H, et al. Profibrogenic effect of high-mobility group box protein-1 in human dermal fibroblasts and its excess in keloid tissues. *Sci Rep*. 2018;8(1):8434. doi:10.1038/s41598-018-26501-6
27. Lierova A, Jelicova M, Nemcova M, et al. Cytokines and radiation-induced pulmonary injuries. *J Radiat Res*. 2018;59(6):709-753. doi:10.1093/jrr/rry067
28. Wang L, Zhang J, Wang B, Wang G, Xu J. Blocking HMGB1 signal pathway protects early radiation-induced lung injury. *Int J Clin Exp Pathol*. 2015;8(5):4815-4822.
29. Song S, Ji Y, Zhang G, et al. Protective effect of atazanavir sulphate against pulmonary fibrosis in *vivo* and in *vitro*. *Basic Clin Pharmacol Toxicol*. 2018;122(2):199-207. doi:10.1111/bcpt.12871
30. Nakazawa Y, Ohtsuka S, Nakahashi-Oda C, Shibuya A. Cutting edge: involvement of the immunoreceptor CD300c2 on alveolar macrophages in bleomycin-induced lung fibrosis. *J Immunol*. 2019;203(12):3107-3111. doi:10.4049/jimmunol.1900890
31. Wang Q, Wang J, Wang J, et al. HMGB1 induces lung fibroblast to myofibroblast differentiation through NF-κB-mediated TGF-β1 release. *Mol Med Rep*. 2017;15(5):3062-3068. doi:10.3892/mmr.2017.6364
32. Mei Z, Tian X, Chen J, et al. α7-nAchR agonist GTS-21 reduces radiation-induced lung injury. *Oncol Rep*. 2018;40(4):2287-2297. doi:10.3892/or.2018.6616
33. Abdel-Aziz AM, Fathy EM, Hafez HM, Ahmed AF, Mohamed MZ. TLR4/MyD88/NF-κB signaling pathway involved in the protective effect of diacerein against lung fibrosis in rats. *Hum Exp Toxicol*. 2023;42:9603271231200213. doi:10.1177/09603271231200213
34. Chung EJ, White AO, Citrin DE. Methods to assess radiation-induced fibrosis in mice. *Methods Cell Biol*. 2023;180:113-126. doi:10.1016/bs.mcb.2023.02.013
35. Cui M, Xiao H, Li Y, et al. Faecal microbiota transplantation protects against radiation-induced toxicity. *EMBO Mol Med*. 2017;9(4):448-461. doi:10.15252/emmm.201606932
36. Wu H, Esteve E, Tremaroli V, et al. Metformin alters the gut microbiome of individuals with treatment-naive type 2 diabetes, contributing to the therapeutic effects of the drug. *Nat Med*. 2017;23(7):850-858. doi:10.1038/nm.4345
37. Chioma OS, Mallott EK, Chapman A, et al. Gut microbiota modulates lung fibrosis severity following acute lung injury in mice. *Commun Biol*. 2022;5(1):1401. doi:10.1038/s42003-022-04357-x
38. Yang T, Guan Q, Shi JS, Xu ZH, Geng Y. Metformin alleviates liver fibrosis in mice by enriching Lactobacillus sp. MF-1 in the gut microbiota. *Biochim Biophys Acta, Mol Basis Dis*. 2023;1869(5):166664. doi:10.1016/j.bbadis.2023.166664
39. Sorbara MT, Littmann ER, Fontana E, et al. Functional and genomic variation between human-derived isolates of Lachnospiraceae reveals inter- and intra-species diversity. *Cell Host Microbe*. 2020;28(1):134-146. doi:10.1016/j.chom.2020.05.005
40. Guo H, Chou WC, Lai Y, et al. Multi-omics analyses of radiation survivors identify radioprotective microbes and metabolites. *Science*. 2020;370(6516):eaay9097. doi:10.1126/science.aay9097
41. Zhang JY, Xiao J, Xie B, et al. Oral metformin inhibits choroidal neovascularization by modulating the gut-retina Axis. *Invest Ophthalmol Vis Sci*. 2023;64(15):21. doi:10.1167/iovs.64.15.21
42. Wabitsch S, McCallen JD, Kamenyeva O, et al. Metformin treatment rescues $CD8^+$ T-cell response to immune checkpoint inhibitor therapy in mice with NAFLD. *J Hepatol*. 2022;77(3):748-760. doi:10.1016/j.jhep.2022.03.010